THE JOURNAL OF PHYSICAL CHEMISTRY Letters

pubs.acs.org/JPCL

Active Role of a Color Indicator in Buoyancy-Driven Instabilities of Chemical Fronts

C. Almarcha,[†] P. M. J. Trevelyan,[†] L. A. Riolfo,[‡] A. Zalts,[§] C. El Hasi,[§] A. D'Onofrio,[‡] and A. De Wit*,[†]

[†]Nonlinear Physical Chemistry Unit, CP 231, Faculté des Sciences, Université Libre de Bruxelles (ULB), Campus Plaine, 1050 Brussels, Belgium, [‡]Grupo de Medios Porosos, Facultad de Ingeniería, Universidad de Buenos Aires, Av. Paseo Colón 850, 1063 Buenos Aires, Argentina, and [§]Universidad Nacional de General Sarmiento, Juan M. Gutiérrez 1150 (B1613GSX) Los Polvorines, Provincia de Buenos Aires, Argentina

ABSTRACT Chemical reactions are able to trigger hydrodynamic flows by changing the density of the solutions across reactive interfaces. In this work, an experimental study of the buoyancy-driven hydrodynamic instabilities that can occur when two miscible reactive solutions of an acid−base system are put in contact in the gravity field shows that the patterns observed and the instabilities taking place strongly depend on the presence of a color indicator. A reaction−diffusion−convection model explains how the color indicator can modify the instability scenarios by affecting the density of the solutions and allows one to numerically recover the observed experimental patterns. The present work clearly demonstrates that color indicators should therefore be used with caution in experimental works devoted to analyze reaction−diffusion−convection patterns and instabilities.

SECTION Surfaces, Interfaces, Catalysis

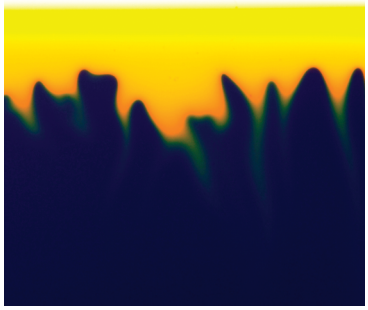

Chemical reactions can actively influence hydrodynamic flows or even more be at the very source of hydrodynamic instabilities. This occurs, for example, if the chemical reaction influences the density, surface tension, or viscosity of the solution across a given interface. Such interfaces exist in reactive systems either if two solutions, each containing one reactant, are initially put in contact, or if specific reactions coupled to diffusion generate self-sustained chemical fronts. Numerous works have analyzed chemo-hydrodynamic patterns developing around autocatalytic fronts.[1−4] Much interest has also been devoted to analyze convective patterns influenced or fully triggered by simple reactions when two reactive solutions are brought into contact.[5,6] Indeed, this situation underlies numerous applications in fields as diverse as earth mantle dynamics,[7] chemical engineering,[8,9] or CO_2 sequestration,[10] to name a few. In the case of a stratification of a solution put on top of another one in the gravity field, convective flows can be triggered by an unfavorable density stratification. This occurs, for instance, if a heavier solution overlies a lighter one, like in the Rayleigh−Taylor instability,[11] or if the two involved chemical species have different diffusion coefficients, like in double diffusive instabilities.[12,13] In the presence of chemical reactions, these sources of instabilities can develop when the reactants diffuse, meet, and react.

Recently, controlled experiments have analyzed such buoyancy-driven patterns triggered by chemical reactions in both immiscible[8,9,14,15] or miscible[16,17] solutions. In some cases, the convective instabilities are studied by adding a color indicator in the solution in order to directly visualize the chemo-hydrodynamic patterns.[8,16] The underlying hypothesis in the use of such color indicators for visualization purposes is that their effect on the dynamics is negligible. However, experiments on buoyancy-driven instabilities of acid−base fronts have recently shown different dynamics depending on whether a color indicator is used[16] or not.[17]

In this context, it is the objective of this letter to show by a combined experimental, theoretical, and numerical approach that color indicators can actually play an active role in buoyancy-driven instabilities of miscible reactive fronts. Indeed, their presence can modify the density profile in the system and therefore change the convective flows triggered by density gradients in the gravity field. To demonstrate this, we first present experimental observations that clearly show the influence of a color indicator on the chemo-hydrodynamic patterns around acid−base fronts. We next develop a reaction−diffusion−convection (RDC) model of the problem incorporating reactions between the chemical species put in contact as well as between these chemical species and the color indicator. These reaction steps are coupled to diffusion and convection processes through a concentration-dependent density term appearing in the evolution equation for the fluid velocity. On the basis of the underlying density profiles, reconstructed using large time asymptotic

Received Date: December 16, 2009
Accepted Date: January 19, 2010

DOI: 10.1021/jz900418d | *J. Phys. Chem. Lett.* **2010**, *1*, 752–757

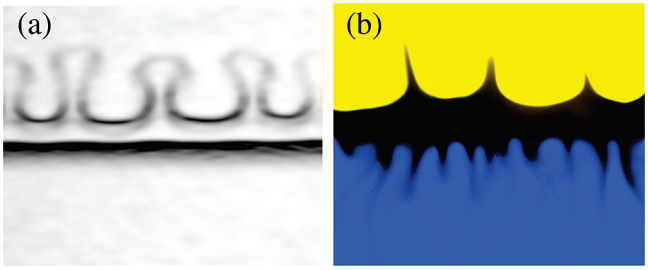

Figure 1. (a) 1 M HCl and 1 M NaOH in the absence of any color indicator; field of view 1.2 cm wide, time $t = 60$ s, $h = 0.5$ mm. In (b) 0.01 M HCl and 0.01 M NaOH in the presence of 0.01 M Bromocresol green; field of view 2.5 cm wide, time $t = 200$ s, $h = 1$ mm.

concentration profiles for all of the species involved (including the color indicator if present), we discuss the various possible sources of convective destabilization of the acid−base front and explain the instabilities observed in the experiments. Finally, we compare the patterns obtained by simulations of the full nonlinear RDC model with those obtained experimentally.

The experimental setup consists of a vertically orientated Hele−Shaw cell (two glass plates separated by a thin gap width h) filled with the reactive solutions of interest. The initial condition inside the cell is a horizontal flat interface separating a solution of reactant A on top of another miscible solution of reactant B. This initial condition can be obtained by putting in contact two half cells, each filled with a different solution.[16] An alternative is to use, like here, a specific device developed for the study of interfacial instabilities with injection into the cell from the top and the bottom and extraction of excess solutions by means of two exhaust sites on the sides.[18] Once the injection is stopped, the experiment starts, and the dynamics is tracked inside the cell either by direct visualization in the presence of a color indicator[16] or, in the absence of it, by interferometry[17] or shadowgraphy like here.

If an aqueous solution of HCl is put on top of an equimolar aqueous solution of NaOH in the absence of any color indicator,[17] the system initially features a stable stratification of light fluid over a heavy one, as the density of the HCl solution is smaller than that of the NaOH one for equal concentrations.[19] Visualization by shadowgraphy, however, shows a convective destabilization of the system in the form of plumes ascending *above* the initial contact line (Figure 1a). No convection is obtained in the lower alkaline layer where the reaction front (seen in Figure 1a as the dark horizontal line), moves downward without deformation. High concentrations were used to enhance the contrast and to obtain a sufficiently small wavelength at onset. Indeed, for a fixed ratio in initial concentrations, the pattern and the dynamics are self-similar with characteristic length and time scales decreasing when the concentrations increase.[17]

If the same experiment is performed with Bromocresol green color indicator added either in the basic solution only[16] or in both solutions like in Figure 1b, the pattern obtained is fundamentally different. Smaller concentrations are used for visualization purposes. The acid and base solutions then appear yellow and blue, respectively. Convection still appears in the acid layer, but an additional cellular deformation, visualized within the intermediate zone where the color changes, is observed around the reaction front in the lower layer and is seen to invade the alkaline solution in the course of time. This is strikingly different from the situation obtained in the absence of the color indicator, which indicates that the color indicator actually plays an active role in the dynamics.

In order to confirm this assertion, additional experiments have been performed where a solution of HCl at initial concentration a_0 is now put on top of an aqueous solution containing only the color indicator in its blue basic form at initial concentration i_0, in the absence of NaOH. The acid is introduced either at the same concentration 0.01 M as the color indicator so that the ratio of initial concentrations $r = a_0/i_0 = 1$ (Figure 2a) or 10 times more concentrated ($r = 10$) (Figure 2b). The acidic form of the color indicator looks orange here instead of yellow as a light source weaker than the one in Figure 1b has been used. For $r = 10$, yellow plumes appear in the upper layer, indicating a local decrease in the density above the initial contact line. At both low and high concentrations of the acid, a modulation of the reaction front also appears in the lower layer between the orange acidic solution and the dark blue basic solution, showing that convection takes place close to the reaction zone. This clearly indicates that the convective destabilization of the reaction front in the lower layer, when it contains both NaOH and a color indicator as observed in ref 16 and in Figure 1b, can come from the presence of the color indicator only.

To understand the active role of the color indicator in the observed convective patterns, we now provide a theoretical description of the dynamics when an acidic solution of A is put in contact with a miscible basic solution of B in the presence of a color indicator. The acid and base react according to the neutralization scheme 1 to form a salt S. The color indicator can be present in its acidic form J or its basic form I. The basic form of the color indicator I can react with the acid A to give J and the salt S according to scheme 2. Also J can react with the base B to form I as in 3. Thus we consider the following three reactions:

$$\mathrm{A} + \mathrm{B} \rightarrow \mathrm{S} \tag{1}$$

$$\mathrm{A} + \mathrm{I} \rightarrow \mathrm{J} + \mathrm{S} \tag{2}$$

$$\mathrm{B} + \mathrm{J} \rightarrow \mathrm{I} \tag{3}$$

For simplicity, we will consider these reactions as irreversible, which is justified with a 10^{-7} precision for molar concentrations of strong acid A and base B.

The buoyancy instabilities we are studying are related to changes in the local density ρ, which, for diluted solutions, is assumed to vary linearly with the concentration of the solutes as

$$\rho(a,b,s,i,j) = \rho_0(1 + \alpha_A a + \alpha_B b + \alpha_S s + \alpha_I i + \alpha_J j) \tag{4}$$

DOI: 10.1021/jz900418d | J. Phys. Chem. Lett. 2010, 1, 752–757

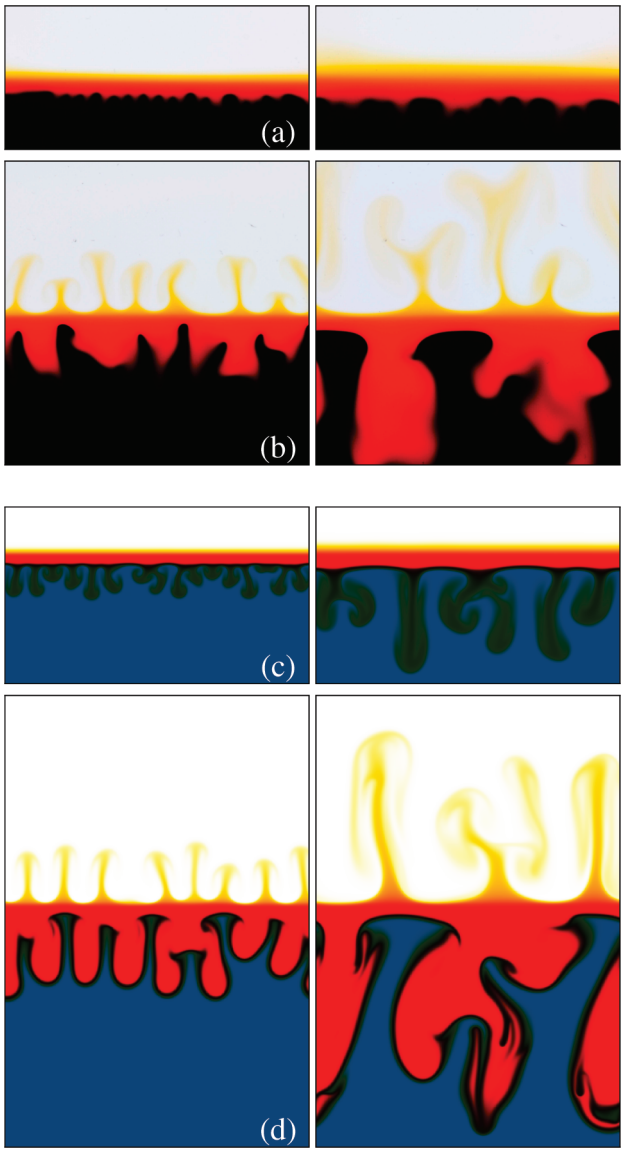

Figure 2. Convective patterns when a 0.01 M solution of Bromocresol green is put under a solution of HCl with (a) $r = 1$ and (b) $r = 10$; width is 3 cm; $h = 1$ mm. First and second columns correspond to $t = 25$ s and $t = 75$ s, respectively. Related numerical simulations, (c) $r = 1$ and (d) $r = 10$, dimensionless times are 2000 (left) and 6000 (right); width is 1024.

ρ_0 is the density of the solvent (here water), $\alpha_\gamma = (1/\rho_0)(\partial\rho/\partial\gamma)$ is the solutal expansion coefficient of species γ, while a, b, s, i, and j are the concentrations of species A, B, S, I, and J, respectively. Although acid−base reactions are typically exothermic, we have checked in ref 17 that temperature plays virtually no role on the dynamics studied here in a Hele−Shaw cell. Because of the high diffusivity of heat, the thermal density gradients can indeed be shown to be small compared to the solutal density gradients.[17]

The RDC model describing the dynamics in the Hele−Shaw cell couples the evolution equations for the concentrations (5c−5g) to Darcy's equation for the fluid velocity $\underline{u}$ in the Boussinesq approximation (5a) through the state eq 4 as

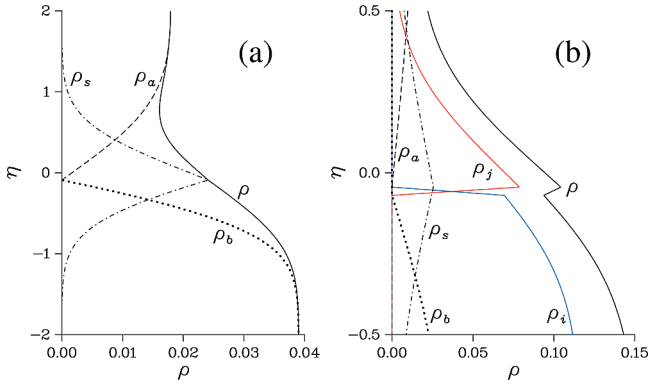

Figure 3. Sketch of the total density and of the contribution to it $\rho_\gamma = \alpha_\gamma\gamma$ of species γ when a 1 M solution of HCl is put on top of a 1 M solution of NaOH (a) without color indicator and (b) with a 0.3 M solution of color indicator in the lower layer when $\alpha_J = 0.465 > \alpha_I = 0.385$. $D_I = D_J = 0.45\ 10^{-9}$ m^2/s.

$$\frac{\mu}{K}\underline{u} = -\nabla p + \rho(a,b,s,i,j)\underline{g} \tag{5a}$$

$$\nabla\cdot\underline{u} = 0 \tag{5b}$$

$$a_t + \underline{u}\cdot\nabla a = D_A\nabla^2 a - k_1 ab - k_2 ai \tag{5c}$$

$$b_t + \underline{u}\cdot\nabla b = D_B\nabla^2 b - k_1 ab - k_3 bj \tag{5d}$$

$$s_t + \underline{u}\cdot\nabla s = D_S\nabla^2 s + k_1 ab + k_2 ai \tag{5e}$$

$$i_t + \underline{u}\cdot\nabla i = D_I\nabla^2 i - k_2 ai + k_3 bj \tag{5f}$$

$$j_t + \underline{u}\cdot\nabla j = D_J\nabla^2 j + k_2 ai - k_3 bj \tag{5g}$$

where $\underline{g}$ is the gravitational acceleration, p is the pressure, $K = h^2/12$ is the permeability, while μ and D_γ are the viscosity of the solvent and the diffusion coefficient of species γ assumed to be constant, respectively. k_1, k_2, and k_3 are the kinetic constants of reactions 1, 2, and 3, respectively. Although we deal here with ionic solutions as the strong acid A and base B dissociate into ions in water, we suppose as a first approximation that each ion diffuses with its counterion, so that A stands for the pair (H^+ Cl^-) in the case of a solution of HCl for instance.

In order to gain insight into the origin of the instabilities, the density profile (eq 4) along the vertical axis can be constructed on the basis of reaction−diffusion concentration profiles obtained by numerical integration of eqs 5c−5g in the absence of convection ($\underline{u} = \underline{0}$). At large times compared to the reaction time, the profiles are self-similar, with a constant amplitude and with lengths scaling like $t^{1/2}$. Assuming instantaneous reactions (infinite reaction constants), the zone of coexistence of A and B is infinitely thin and corresponds to the location of the reaction front in the following. Large time asymptotic solutions are calculated using a similar approach to ref 20 and are reported in Figure 3 along η, the vertical coordinate rescaled by $(4D_A t)^{1/2}$. To model the experiments performed here, the physical properties of A, B, and S are

DOI: 10.1021/jz900418d | J. Phys. Chem. Lett. 2010, 1, 752–757

taken as those of HCl, NaOH, and NaCl, respectively: α_A = 0.018 M^{-1}, α_B = 0.039 M^{-1}, α_S = 0.038 M^{-1}, D_A = 3.0 $10^{-9}m^2/s$, D_B = 1.9 $10^{-9}m^2/s$, D_S = 1.5 $10^{-9}m^2/s$.[19]

The density profiles are first reported in Figure 3a for equal initial concentrations of A and B in the absence of a color indicator. As species A diffuses downward faster than S diffuses upward, the net flux of mass is negative in a depleted zone of the upper layer where a local minimum of density appears ($\eta \approx 0.78$). This leads to a stratifically unstable zone in the upper layer ($\eta > 0.78$) that triggers convection above the position of initial contact. Such a stratifically unstable zone does not appear in the lower layer. The reaction front, moving downward in the lower layer, is in a stratifically stable region, so it remains planar as seen in Figure 1a and in ref 17.

When a color indicator is added to the lower alkaline solution, the density profile is far different, as seen in Figure 3b where the ratio of initial concentrations is the same as in ref 16, but concentrations are 100 times larger to better compare to Figure 3a. First of all, the color indicator is usually a big molecule with a large molecular weight and a solutal expansion coefficient larger than that of the other species. The density is therefore strongly increased (Figure 3b) in the zone where the color indicator (whether in its acidic or basic form) is present with regard to the pure HCl/NaOH profile (Figure 3a).

Besides the reaction front where A reacts with B, there is an upper zone where the color indicator has diffused and is in contact with the acid A. According to reaction 2, the color indicator is there present in its acidic form J, which contributes with a weight ρ_j to the density. In the lower alkaline region, the color indicator reacts according to reaction 3 and is thus present essentially in its basic form I, giving a contribution ρ_i to the density profile. The zone of approximately linear transition from one form of the color indicator to the other one is small compared to the characteristic length of the density variation ($-1 < \eta < 1$) but large compared to the reaction front thickness. It can play a leading role in the destabilization, particularly if the acidic and basic forms of the color indicator I and J do not have the same physical properties.

If, for instance, α_J is slightly larger than α_I for $D_J = D_I$ (J slightly heavier than I at the same concentration), a locally unstable zone where a heavy fluid lies on top of a light fluid is obtained, as reported in the density profile of Figure 3b. This unstable density stratification lies in the neighborhood of the reaction front that could then be perturbed. The same kind of locally unstable stratification can be obtained at equal expansion coefficients when I and J have different diffusion coefficients (if $D_J < D_I$ for instance). In this case again, convection may appear around the reaction front.

If $\alpha_J < \alpha_I$, as is the case for Bromocresol green for which we have measured $\alpha_I = (0.385 \pm 0.008)\ M^{-1}$ and $\alpha_J = (0.370 \pm 0.008)\ M^{-1}$, and if we suppose $D_J \sim D_I$, the instability scenario is different but also leads to convection, as seen in Figure 2a–d. There, the upper acid solution is lighter than the lower solution of Bromocresol green so that a Rayleigh–Taylor instability cannot happen. As the acid diffuses faster than the indicator, the reaction front where reaction 2 takes place moves downward. An instability in that case appears due to differential diffusion effects. The density profiles are plotted in Figure 4 for the two ratios r = 1 and 10 corresponding to the cases studied experimentally in Figure 2a,b.

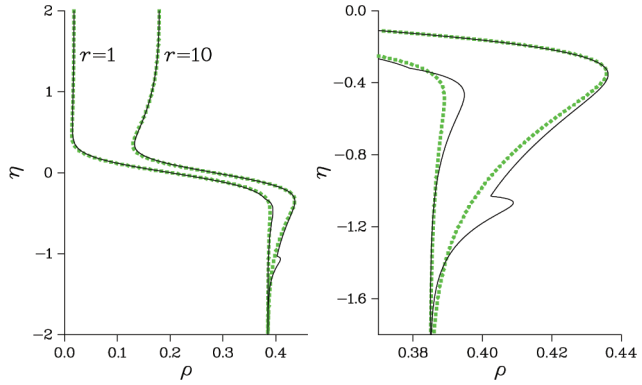

Figure 4. Sketch of the density variations when a 0.01 M (r = 1) or 0.1 M (r = 10) solution of HCl is put on top of a 0.01 M solution of Bromocresol green indicator. The green dashed lines are the nonreactive cases. A zoom in is reported in the right panel.

For equal initial concentrations of the acid and the indicator (r = 1), the density has a local minimum in the upper layer ($\eta \approx 0.57$) and a local maximum in the lower layer ($\eta \approx -0.47$). Therefore, two unstable zones where a heavy fluid lies on top of a lighter one are obtained (Figure 4). The depletion zone in the upper layer due to the fast diffusion of the acid downward is of very small amplitude and leads to very weak convection. However, the related increase in density due to the accumulation of the salt S inside the lower layer is stronger in the lower part. One can therefore expect a stronger convection in that region located below the initial contact line. This is coherent with what is observed experimentally (Figure 2a).

If now the acid in the upper layer is initially 10 times more concentrated than the color indicator (r = 10), the density has one local minimum in the upper layer ($\eta \approx 0.35$) and two local maxima in the lower layer ($\eta \approx -0.35$ and $\eta \approx -1.07$) as seen in Figure 4. The intensity of the minimum in density (depletion zone) above the initial contact line and of the maximum below it is now larger as more acid is present initially. If we compare this density profile with the one obtained without any reaction between A and I (dotted curve), we see that the only difference is the presence of the second small local maximum in the lower part, inside a stratifically unstable region. We can conclude that, in this particular situation, the convection will be roughly the same as in the nonreactive situation: the density profile is nearly antisymmetric with respect to the initial contact line. Convection with almost equal strengths can therefore develop on both sides of the initial contact line as observed in experiments (Figure 2b).

We have thus seen that various instability scenarios can be expected when an acid is put on top of a color indicator (Figure 4) or on top of a strong base in the presence or not of a color indicator (Figure 3). In all cases, convection can set in and perturb the dynamics either in the upper layer, in the lower one, or in both of them. Comparison of Figure 3 and Figure 4 allows one to understand that the convective patterns observed when a lighter HCl solution is put above a heavier

DOI: 10.1021/jz900418d | J. Phys. Chem. Lett. 2010, 1, 752–757

solution of NaOH in the presence of bromocresol green[16] result from a combination of the convective destabilization obtained when A is put in contact with B in the absence of color indicator and of the situation when A is put in contact with the color indicator in the absence of a strong base.

In order to check the instability scenarios discussed above and compare the resulting nonlinear dynamics to experiments, the full nonlinear model (5) has been solved in two dimensions by a pseudospectral scheme[21] adapted to take multiple diffusing species and reactions into account. The program is based on Fourier transforms of the stream function, derived from Darcy's law, and of the concentrations. The initial condition for the concentrations of the species put in contact are step functions with the addition of a small amount of noise in order to control the emergence of the instability within a zero stream function field. The concentrations, speed, length, and time are nondimensionalized by a_0, $u_c = \rho_0 g K \alpha_A a_0/\mu$, $l_c = D_A/u_c$, and $t_c = D_A/u_c^2$, respectively, as in ref 17. We took $D_I = D_J = 0.15\ 10^{-9}$ m^2/s, and the kinetic constants k_i have been chosen equal and large such that $k_i a_0 t_c = 1$. The resulting patterns are reported for two different times in Figure 2c,d. The color scale has been chosen to match the pure acid on white and the pure color indicator on dark blue and extrapolating in between, assuming that the absorbance of light varies as a function of the concentrations according to Beer−Lambert's law. The most unstable wavelength and the onset time of the instability are seen to drastically change with D_I and D_J. The nonlinear numerical patterns are in good qualitative agreement with the experimental ones.

In conclusion, we have demonstrated the active role that a color indicator can play on buoyancy-driven instabilities of acid−base fronts. By modifying the density profile in the system, a color indicator can influence or trigger convection in a chemical system, leading to various different patterns depending on the initial concentration ratio of the species put in contact. Let us note that a very large number of different possible sources of convection is expected if diffusion and/or solutal expansion coefficients are different for all of the involved species. As the precise values of the different pro perties of all the involved species need to be known, it remains difficult to determine which exact scenario is at hand. However, this study clearly demonstrates that pattern formation due to the coupling of chemical reactions with buoyancy-driven convection can be tremendously affected by the use of a color indicator for visualization purposes. Such color indicators should therefore be used with caution in experimental works devoted to analyze RDC patterns and instabilities.

AUTHOR INFORMATION

Corresponding Author:

*To whom correspondence should be addressed. E-mail: adewit@ulb.ac.be.

ACKNOWLEDGMENT We thank K. Eckert, Y. De Decker and J.-M. Frère for fruitful discussions. A.D. acknowledges Prodex, FNRS, Multiflow, and the Faculté des Sciences (ULB) for financial support. Our collaboration has benefited from a CONICET (Argentina)/FRS-FNRS (Belgium) bilateral cooperation programme.

REFERENCES

(1) De Wit, A. Miscible density fingering of chemical fronts in porous media: Nonlinear simulations. *Phys. Fluids* **2004,** *16*, 163–175.
(2) Casado, G. G.; Tofaletti, L.; Müller, D.; D'Onofrio, A. Rayleigh−Taylor instabilities in reaction−diffusion systems inside Hele−Shaw cell modified by the action of temperature. *J. Chem. Phys.* **2007,** *126*, 114502.
(3) Rongy, L.; Schuszter, G.; Sinkó, Z.; Tóth, T.; Horváth, D.; Tóth, A.; De Wit, A. Influence of thermal effects on buoyancy-driven convection around autocatalytic chemical fronts propagating horizontally. *Chaos* **2009,** *19*, 023110.
(4) Macias, L.; Müller, D.; D'Onofrio, A. Influence of porosity on Rayleigh−Taylor instabilities in reaction−diffusion systems. *Phys. Rev. Lett.* **2009,** *102*, 094501.
(5) Citri, O.; Kagan, M. L.; Kosloff, R.; Avnir, D. Evolution of chemically induced unstable density gradients near horizontal reactive interfaces. *Langmuir* **1990,** *6*, 559–564.
(6) Avnir, D.; Kagan, M. L. The evolution of chemical-patterns in reactive liquids, driven by hydrodynamic instabilities. *Chaos* **1995,** *5*, 589–601.
(7) Davaille, A. Simultaneous generation of hotspots and superswells by convection in a heterogeneous planetary mantle. *Nature* **1999,** *402*, 756–760.
(8) Eckert, K.; Acker, M.; Shi, Y. Chemical pattern formation driven by a neutralization reaction. I. Mechanism and basic features. *Phys. Fluids* **2004,** *16*, 385–399.
(9) Wylock, C.; Dehaeck, S.; Rednikov, A.; Colinet, P. Chemo-hydrodynamical instability created by CO_2 absorption in an aqueous solution of $NaHCO_3$ and Na_2CO_3. *Microgravity Sci. Technol.* **2008,** *20*, 171–175.
(10) Riaz, A.; Hesse, M.; Tchelepi, H. A.; Orr, F. M., Jr. Onset of convection in a gravitationally unstable diffusive boundary layer in porous media. *J. Fluid Mech.* **2006,** *548*, 87–111.
(11) Fernandez, J.; Kurowski, P.; Petitjeans, P.; Meiburg, E. Density-driven unstable flows of miscible fluids in a Hele−Shaw cell. *J. Fluid Mech.* **2002,** *451*, 239–260.
(12) Turner, J. S. *Buoyancy Effects in Fluids*; Cambridge University Press: Cambridge, U.K., 1979.
(13) Griffiths, R. W. Layered double-diffusive convection in porous media. *J. Fluid Mech.* **1981,** *102*, 221–248.
(14) Eckert, K.; Grahn, A. Plume and finger regimes driven by an exothermic interfacial reaction. *Phys. Rev. Lett.* **1999,** *82*, 4436–4439.
(15) Bratsun, D. A.; Shi, Y.; Eckert, K.; De Wit, A. Control of chemo-hydrodynamic pattern formation by external localized cooling. *Europhys. Lett.* **2005,** *69*, 746–752.
(16) Zalts, A.; El Hasi, C.; Rubio, D.; Ureña, A.; D'Onofrio, A. Pattern formation driven by an acid−base neutralization reaction in aqueous media in a gravitational field. *Phys. Rev. E* **2008,** *77*, 015304.
(17) Almarcha, C.; Trevelyan, P. M. J.; Grosfils, P.; De Wit, A. Chemically driven hydrodynamic instabilities. *Phys. Rev. Lett.* **2010,** *104*, 044501.
(18) Shi, Y.; Eckert, K. A novel Hele−Shaw cell design for the analysis of hydrodynamic instabilities in liquid−liquid systems. *Chem. Eng. Sci.* **2008,** *63*, 3560–3563.
(19) *CRC Handbook of Chemistry and Physics*, 59th edition; Weast, R. C.; Astle, M. J., Eds.; CRC Press: Boca Raton, FL, 1979.

DOI: 10.1021/jz900418d | *J. Phys. Chem. Lett.* **2010,** *1*, 752–757

(20) Sinder, M.; Pelleg, J. Asymptotic properties of a reversible $A + B \leftrightarrow C$ reaction−diffusion process with initially separated reactants. *Phys. Rev. E* **2000,** *62*, 3340–3348.
(21) Tan, C. T.; Homsy, G. M. Simulation of nonlinear viscous fingering in miscible displacement. *Phys. Fluids* **1988,** *31*, 1330–1338.

DOI: 10.1021/jz900418d | *J. Phys. Chem. Lett.* **2010,** *1*, 752–757